Soft Matter

PAPER

View Article Online
View Journal | View Issue

Cite this: *Soft Matter*, 2021, **17**, 3937

Shear modulus and yield stress of foams: contribution of interfacial elasticity

Annika R. Völp * and Norbert Willenbacher

Received 21st December 2020,
Accepted 6th March 2021

DOI: 10.1039/d0sm02246b

rsc.li/soft-matter-journal

The link between interfacial elasticity of foaming solutions and the elasticity and yield stress of their aqueous foams is probed for a variety of surfactant, block-copolymer, protein, food, and particle-stabilized (Pickering) foams. We measured interfacial tension σ and interfacial elastic moduli of foaming solutions in dilation E_∞ as well as in shear G_i' at concentrations suitable for foaming and compared them to the shear modulus and yield stress of corresponding foams normalized by bubbles' Sauter radius R_{32} and foams' gas volume fraction. The interfacial shear modulus was only measurable for the foaming solutions including proteins or nanoparticles. For these systems the foam shear modulus scaled reasonably well with $(\sigma + 2G_i')/R_{32}$. The interfacial dilational modulus was accessible for all investigated systems and the foam shear modulus as well as yield stress scaled with a generalized Laplace pressure $(\sigma + 2E_\infty)/R_{32}$. But foams stabilized by nanoparticles or aggregated proteins exhibited even higher shear modulus and yield stress values not captured by the proposed scaling with the generalized Laplace pressure and also show an unexpectedly high dependence of these characteristics on the gas volume fraction. We attribute this to attractive forces between particles and/or structure formation across the lamellae that become increasingly dominant as the lamellae narrow down during foam drainage.

Introduction

Foams and emulsions are complex disperse systems with unique texture and rheology. Though the individual phases are purely viscous, foams and emulsions display viscoelastic behavior when the dispersed phase exceeds the maximum packing fraction and the bubbles or droplets start to deform. Such foams and emulsions exhibit a yield stress, *i.e.* a critical stress at which neighboring bubbles or droplets rearrange topologically. Princen[1,2] concluded from a two-dimensional model of equally-sized hexagonal cells that the elastic modulus G' and yield stress τ_y of foams or emulsions exceeding the maximum packing fraction φ_c scale with the Laplace pressure within the cells, *i.e.* the ratio of interfacial tension σ and bubble or droplet radius R. For the two-dimensional case an analytical solution for the dependence of these rheological parameters on the dispersed volume fraction φ was derived. Based on experiments with polydisperse emulsions stabilized by a small molecular weight surfactant (ammonium laureth sulfate), Princen and Kiss[3] established an empirical dependence of rheological parameters on $(\varphi - \varphi_c)$ using $\varphi_c = 0.712$ close to the critical volume fraction $\varphi_c = 0.74$ of hexagonal close packed monodisperse spheres and suggested to express the bubble or droplet size in terms of the Sauter radius R_{32}. Mason *et al.*[4,5] refined the models suggesting the following semi-empirical equations:

$$G' = a\frac{\sigma}{R_{32}}\varphi(\varphi - \varphi_c) \quad (1)$$

$$\tau_y = k\frac{\sigma}{R_{32}}(\varphi - \varphi_c)^2 \quad (2)$$

Based on experimental data for carefully prepared monodisperse emulsions of silicon oil in water also stabilized with small molecular weight surfactant (sodium dodecylsulphate) they found numerical pre-factors $a = 1.64$ and $k = 0.51$, for the critical gas volume fraction they chose $\varphi_c \approx 0.635$ corresponding to randomly close packed monodisperse spheres. Marze *et al.*[6] confirmed the models to hold true for foams stabilized by small molecular weight surfactants (sodium dodecylsulphate; potassium cocoyl glycinate) and found numerical values $a = 1.53$ and $k = 0.62$, but stated that the elastic modulus of casein stabilized foams was lower than predicted from eqn (1). They related this conflicting behavior to the slower adsorption dynamics of the larger casein molecules, the viscoelasticity of the casein covered interface and thicker interfacial films. Dimitrova and Leal-Calderon[7] found substantially higher shear moduli for hexadecane–water emulsions stabilized with casein, β-lactoglobulin and bovine serum albumin than known for sodium docecyl sulfate. They reported that G' values of those three emulsions increased

Institute for Mechanical Process Engineering and Mechanics: Applied Mechanics, Karlsruhe Institute of Technology, Gotthard-Franz-Str. 3, 76131 Karlsruhe, Germany

with literature values for their corresponding interfacial dilatational elasticity E_A ranging from 9 to 26 mN m^{-1}. Davis *et al.*[8] tried to correlate the yield stress of whey protein foams with the dilatational interfacial elastic modulus of the foaming solution (varying from 15 to 80 mN m^{-1}) at various pH and ionic strength, but did not consider the foams' gas volume fraction nor the bubble size. Lexis and Willenbacher[9] found the elastic moduli of milk protein stabilized foams to increase with the surface elastic modulus in shear (varying from 5 to 100 mN m^{-1}) and in dilation (varying from 0.1 to 80 mN m^{-1}). The shear moduli of these foams exceeded the values predicted by eqn (2) by more than a factor of ten. They also correlated the foams' yield stress with the critical interfacial shear strain at which the interfacial layer structure breaks. Even higher foam elastic modulus and yield stress values, not captured by the correlation between foam and interfacial viscoelastic properties, were found under conditions favoring protein aggregation and were attributed to lamellae spanning structures. Tsibranska *et al.*[10] suggested the bulk elastic modulus of emulsions to scale with interfacial dilatational elastic modulus $E_A > 5$ mN m^{-1} as follows:

$$G' = 1.7\frac{\sigma}{R_{32}}\varphi(\varphi - \varphi_c)(1.5 \lg E_A). \quad (3)$$

However, eqn (5) is based on a limited set of data comprising two hexadecane–water emulsions and one sunflower oil–water emulsion stabilized by saponins. Costa *et al.*[11] investigated the dependency of the complex shear modulus G^* of foams on frequency f and found deviations from the expected $G^* \sim f^{1/2}$ scaling for surfactant mixture solutions with high complex interfacial dilatational moduli E^*. At sufficiently high dilatational frequency exchange between the foaming agent at the interface and in the bulk is prevented and E^* reaches the limiting elasticity $E_\infty = E' = E_A$, while E'' tends to zero.[11] Costa *et al.* assumed that the complex foam modulus G^* is related to the surface tension as well as the interfacial elasticity and suggested $G^* \sim \sigma/R_{32} + E_\infty/R_{32}$, omitting dimensionless pre-factors.

Based on these studies a contribution of the interfacial elasticity to the elastic modulus and yield stress of foams and emulsions should be taken into account. However, this is not considered in the widely used model equations describing foam elasticity and yield stress (eqn (1) and (2)), which were derived from investigations on emulsions and foams stabilized by low molecular weight surfactants lacking in substantial interfacial elasticity. We are not aware of any systematic investigation on the quantitative contribution of the interfacial elasticity to the foam elasticity or yield stress comprising of different types of foaming agents.

We determined the interfacial tension and interfacial elastic moduli of surfactant, block copolymer, and protein solutions, food systems and nanoparticle dispersions in shear as well as in dilation at amphiphile concentrations suitable for foaming. The elastic shear moduli and yield stresses of foams prepared from the same foaming solutions were measured and normalized to the respective bubble Sauter radii and gas volume fractions according to the suggested scaling in eqn(1) and (2). The critical gas volume fraction was set to $\varphi_c \approx 0.635$ as suggested earlier.[6] We correlated normalized shear modulus and yield stress values to the interfacial elasticity data and propose a quantitative contribution of the latter to the foam rheological characteristics yielding a refinement of eqn (1) and (2).

Experimental

Solution preparation and interface characterization

Food systems, aqueous solutions of surfactants, block copolymers and proteins, and dispersions of nanoparticles were prepared as stated in Table 1. For reasons of readability, we refer to all these systems as foaming solutions in the following.

The gas/liquid interfaces of the foaming solutions were characterized in oscillatory dilation at frequencies between 0.05 Hz and 0.67 Hz using the pendant drop method (PAT1, Sintaface) or in case of the block copolymer solutions, at frequencies between 0.1 and 3 Hz using the rising bubble method (Tracker, Teclis Scientific). The drop surface area varied between 10 to 30 mm^2, depending on the maximum drop volume of each foaming solution, respectively. After the equilibrium of the interfacial tension σ was reached, the surface area was dilated in oscillation with a deformation amplitude in the linear viscoelastic regime (max. 10% of the drop surface area) and stepwise increased frequency (see exemplary frequency dependencies of E' in Fig. 5 under footnotes). Since the increase

Table 1 Foaming agents, their concentrations applied for foaming and interfacial elasticity measurements, and the preparation method of the foaming solutions or dispersions

Foaming agent	Concentrations	Preparation
Glycolipid sorbitol decenoate	2 g l^{-1}	As described in ref. 16
Glycolipid glucose 4-methyl-nonanoate	1.2 g l^{-1}	As described in ref. 16
Block copolymer poloxamer 407 (Sigma Aldrich)	0.05, 0.5 and 5 mM poloxamer in 0.1, 50 and 100 mM NaCl, respectively	Dissolved in demineralized water at 20 °C
Block copolymer poloxamer 188 (Sigma Aldrich)	0.5 mM poloxamer in 50 mM NaCl	Dissolved in demineralized water at 20 °C
Guinness stout beer		Degassed; at 20 °C
Whole milk powder (Nestlé)	10 wt%	As described in ref. 17
Bovine serum albumin (Santa Cruz Biotechnology)	1 wt% at pH 6.8 in 0, 10, 50, 100 mM NaCl, respectively, and at pH 4.7 (isoelectric point)	Dissolved in demineralized water at 20 °C
Lupine protein (Prolupin)	1 wt% heat treated, at pH 4. pH 6.8, pH 10, and in 0, 10, 50 mM NaCl, respectively	As described in ref. 18
Hexylamine coated silica nanoparticle 20 nm (LUDOX® TMA, Grace)	2.5 wt% coated with 5, 50, and 70 mM hexylamine in 0, 10, 50 and 100 mM NaCl and 1 mM $CaCl_2$, respectively	As described in ref. 19

in E' with frequency is weak at least for the highest frequencies accessible here, the values obtained at the maximum applicable frequency were treated as the equilibrium values E_∞. In shear, the solution surfaces were stressed in oscillation using a rotational rheometer (DHR3, TA Instruments) equipped with a double wall ring geometry[12] (70 mm ring diameter) at a frequency of 1 Hz and strains in the linear viscoelastic regime to obtain the interfacial elastic shear modulus G_i' (see exemplary strain dependencies of G_i' in Fig. 6 under footnotes). Note, typically the interfacial elastic modulus is smaller in shear than in dilation[13–15] and for several foaming solutions the elastic interfacial shear moduli were below the measuring limit of the rheometer. Furthermore, it should be noted that the interfacial modulus data were determined at the amphiphile concentrations used for foam preparation and thus should be treated as apparent values not necessarily matching the true interfacial elasticity of an amphiphilic monolayer.

Foam preparation and characterization

Foams were produced in glass filter funnels (16–40 μm pore size VitraPOR® Por.4, Robu) perfused by 60 ml nitrogen per minute as described in ref. 16 and 20, except for the reconstituted whole milk foams, which were produced in a commercial milk whipper (Aeroccino4, Nespresso), as described in.[17] Recording of foam age was started once the filter funnel was completely filled with foam and the nitrogen flow was stopped or the whipper stopped the foaming process. The ratios between foam and solution conductivity during free drainage of the foams were measured at the center of the foam column using a rod-shaped electrode with 5 mm measuring gap width connected to a conductivity meter (Inlab731 and SevenCompact S230, Mettler Toledo). The gas volume fraction φ of the foams was calculated from the relative foam conductivity κ as described in ref. 21:

$$\varphi = 1 - \frac{3\kappa(1 + 11\kappa)}{1 + 25\kappa + 10\kappa^2}. \quad (4)$$

The foams' Sauter radius R_{32} was determined from minimum 100 bubbles on images captured in the center of the foam column with an endoscope connected to a CCD camera (TVS80.280.BF6.AD10.2x-Zoom endoscope, Visitool and Lu 160 camera, Lumenera or VH-B55 endoscope and VHX-950F digital microscope, Keyence). The foams were illuminated from outside through the transparent container wall using a 600 lm LED lamp. The bubbles size distribution was automatically determined from the images without further processing using a template matching based bubble detection tool as described elsewhere.[22] The images were screened for similarities with circular templates differing in radius and the Sauter bubble radius R_{32} was calculated from the ensemble of detected bubbles. At specific foam ages corresponding to desired gas volume fractions between 0.85 and 0.95, foams were transferred into the gap of a plate–plate geometry and sheared in oscillation using a rotational rheometer (RheoScope 1, Thermo Fisher Scientific) at 1 Hz frequency and varying stress amplitude between 0.1 and 100 Pa as described in ref. 20. The gap width between the plates, which were 60 mm in diameter and covered with sandpaper to prevent wall slip, was set to 5 or 6 mm, but never less than ten times the maximum bubble diameter. Effects of wave propagation within the gap were negligible as the smallest possible wave length was estimated to be about ten times larger than the gap width even for the smallest G' values measured at the selected oscillation frequency of 1 Hz.[23] As typical for highly concentrated, densely packed foams the frequency independent regime of G' was found at oscillation frequencies around 1 Hz[6] and the measured elastic moduli G' are termed shear moduli G_0. The foam yield stress was either measured with the same plate–plate setup or with a four bladed vane rotor (36 mm diameter, 9 mm height) submerged into the foaming apparatus as described in ref. 17. The shear stress was increased in 12 steps between 0.1 Pa and 100 Pa and the deformation was recorded during a total measuring time of 60 s. The yield stress τ_y was determined from logarithmically plotted deformation *versus* shear stress data using the tangent intersection method.[24] The results shown in the subsequent sections were determined from at least three measurements with freshly prepared foams, the displayed data are average values and the standard deviations are shown as error bars, error propagation was considered where applicable.

Results and discussion

The interfacial tension, σ and the interfacial elastic moduli in shear G_i' and dilation E_∞ of the foaming solutions are displayed in Table 2.

Fig. 1 shows the foam shear moduli normalized to the reciprocal bubble's Sauter radius ${R_{32}}^{-1}$ and $\varphi(\varphi - \varphi_c)$ *versus* the equilibrium interfacial tension σ, the interfacial dilatational modulus E_∞ and the interfacial shear modulus G_i' of the foaming solutions, respectively. The critical gas volume fraction φ_c was set to 0.635 corresponding to randomly packed monodisperse spheres. Preliminary data analysis revealed that it was not feasible to determine φ_c from the measured bubble size distribution as suggested earlier[20] since the experimental uncertainty was too high and would have blurred the correlations between foam rheological quantities and interfacial elasticity of corresponding foaming solutions. The interfacial tension of the foaming agent solutions covers the range from 25 to 70 mN m^{-1}. The interfacial moduli of the same solutions vary in a much broader range from 2 to 200 mN m^{-1} in dilation and from about 10 to 1000 mN m^{-1} in shear.

The normalized shear moduli of the foams show no unique correlation with the equilibrium surface tension (Fig. 1(a)). But clearly, the foam modulus increases monotonically with the dilatational modulus, as can be seen in Fig. 1(b), and according to Fig. 1(c) also with the interfacial shear modulus of the foaming solutions, albeit to a weaker extend. The strong coupling of foam and interfacial modulus is demonstrated covering two orders of magnitude in interfacial modulus values.

Costa *et al.* suggest that the contribution of interfacial tension and interfacial elasticity superimpose linearly. Thus, we propose the following model:

$$G_0 = 1.6\frac{(\sigma + CG_i')}{R_{32}}\varphi(\varphi - \varphi_c). \quad (5)$$

Table 2 Interfacial tension σ (max. 4% error), interfacial elastic moduli in shear G_i' (max. 33% error) and dilation E_∞ (max. 22% error) in mN m^{-1}

Foaming agent		σ	G_i'	E_∞
Sorbitol decenoate		26.6		3.3
Glucose 4-methyl-nonanoate		29.4		5.2
Poloxamer 407				
	0.05 mM Poloxamer + 100 mM NaCl	39.5, 41.1		11.6, 12.5
	0.5 mM Poloxamer + 50 mM NaCl	39.3		10.9
	5 mM Poloxamer + 100 mM NaCl	38.6, 38.2		8.6, 11.1
Poloxamer 188				
	0.5 mM Poloxamer + 50 mM NaCl	44.2		14.7
Guinness stout		44.2		18.7
Milk powder		47		37.3
Bovine serum albumin				
	pH 4.7	53.1	8.8	73.2
	pH 6.8	52.3	12.1	56.6
	+10 mM NaCl	55.6	26.1	45.9
	+50 mM NaCl	55.2		64.8
	+100 mM NaCl	53.7		57.5
	+50 mM KCL	52		21.1
LPI	pH 6.7 20 °C	43.2		31.5
	+10 mM NaCl	42.9		30.7
	+50 mM NaCl	42.7		32.7
	50 °C	41.9		36.4
	70 °C	41.5		42.4
	90 °C	41.3		39.5
	100 °C	42.6		35.5
	pH 4	46.5		24.2
	pH 10	42.5		25.2
TMA	5 mM hexylamine	63.5	58.6	
	50 mM hexylamine	42.3	328	62.5
	+10 mM NaCl	39.6	391	78.3
	+50 mM NaCl	43.8		139
	+100 mM NaCl	40	816	115
	+1 mM $CaCl_2$	55.6		157
	70 mM hexylamine	45.4	212	

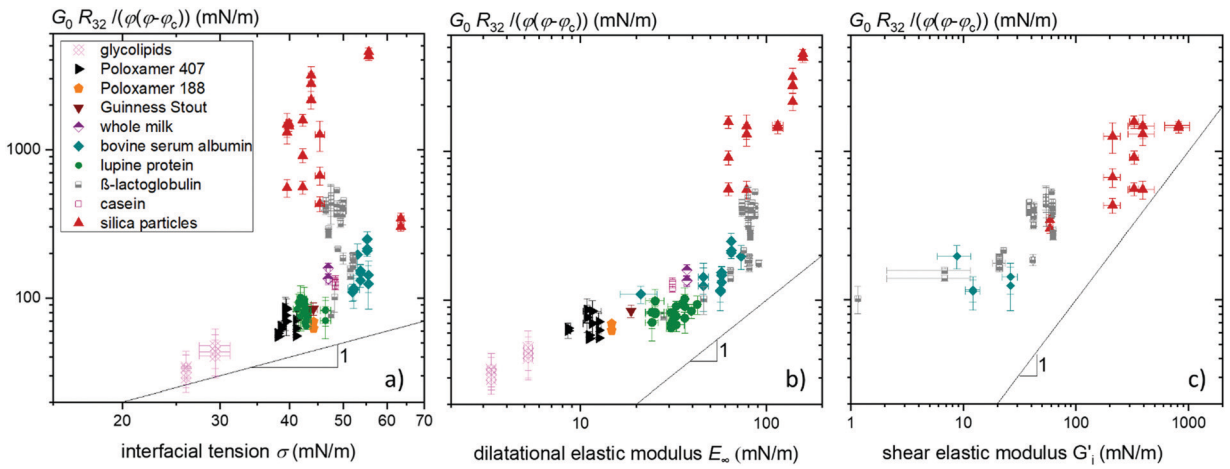

Fig. 1 Foam elastic modulus G_0 normalized to the reciprocal bubble Sauter radius R_{32}^{-1} and $\varphi(\varphi - \varphi_c)$ *versus* (a) interfacial tension σ, (b) interfacial dilatational elastic modulus E_∞ and (c) interfacial shear elastic modulus G_i' of the corresponding foaming solutions. Data for β-lactoglobulin were reused from ref. 9.

where C is a fitting parameter. Eqn (5) reduces to the widely accepted model eqn (1) for $G_i' = 0$, as it is the case for small molecular weight surfactants. Fig. 2 shows the normalized foam moduli *versus* $\sigma + 2G_i'$. With C = 2, eqn (5) fits the data for

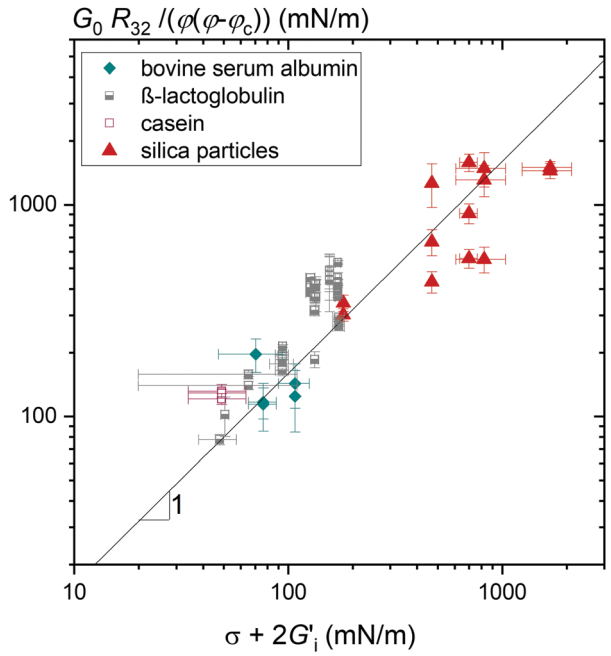

Fig. 2 Foam elastic modulus G_0 normalized by the reciprocal bubble Sauter radius R_{32}^{-1} and $\varphi(\varphi - \varphi_c)$ *versus* the sum of interfacial tension σ and twice the interfacial shear modulus G_i' of the foaming solution. Solid line shows the linear relationship with the pre-factor 1.6. Data for β-lactoglobulin were reused from ref. 9.

animal-based proteins and silica particles very well, covering two orders of magnitude in $\sigma + 2G_i'$ and more than one order of magnitude in G_0. The high interfacial shear elasticity of particle dispersions is attributed to a strong interfacial network and jamming effects, occurring when the interface is sheared or compressed. However, for a given foaming solution. *i.e.* constant $\sigma + 2G_i'$, strong differences between the normalized shear modulus data corresponding to foams with different gas volume fractions indicate additional physical mechanisms contributing to foam elasticity not captured by the interfacial elasticity. Proteins show lower interfacial shear elasticities but also form interfacial networks. This is indicated by the onset of non-linearity of G_i' at deformations $<5\%$ corresponding to network break-up. However, eqn (5) is not applicable to surfactant and block copolymer or lupin protein stabilized foams as these foaming agents do not exhibit measurable interfacial shear elasticities.

Foaming systems that do not show measurable interfacial shear moduli G_i' still exhibit high frequency dilatational elastic moduli E_∞. The dependence of normalized foam moduli and yield stresses on $\sigma + 2E_\infty$ are depicted in Fig. 3(a) and (b), respectively. The correlation between the foam elasticity and $\sigma + 2E_\infty$ is quite distinct for a broad variety of foaming agents. The foam yield stress also correlates with $\sigma + 2E_\infty$ but less clearly.

Solving the differential equation for a sphere

$$E_A = A\frac{d\sigma}{dA} = \frac{R}{2}\frac{d\sigma}{dR} \quad (6)$$

yields the radius-dependent interfacial tension of a spherical

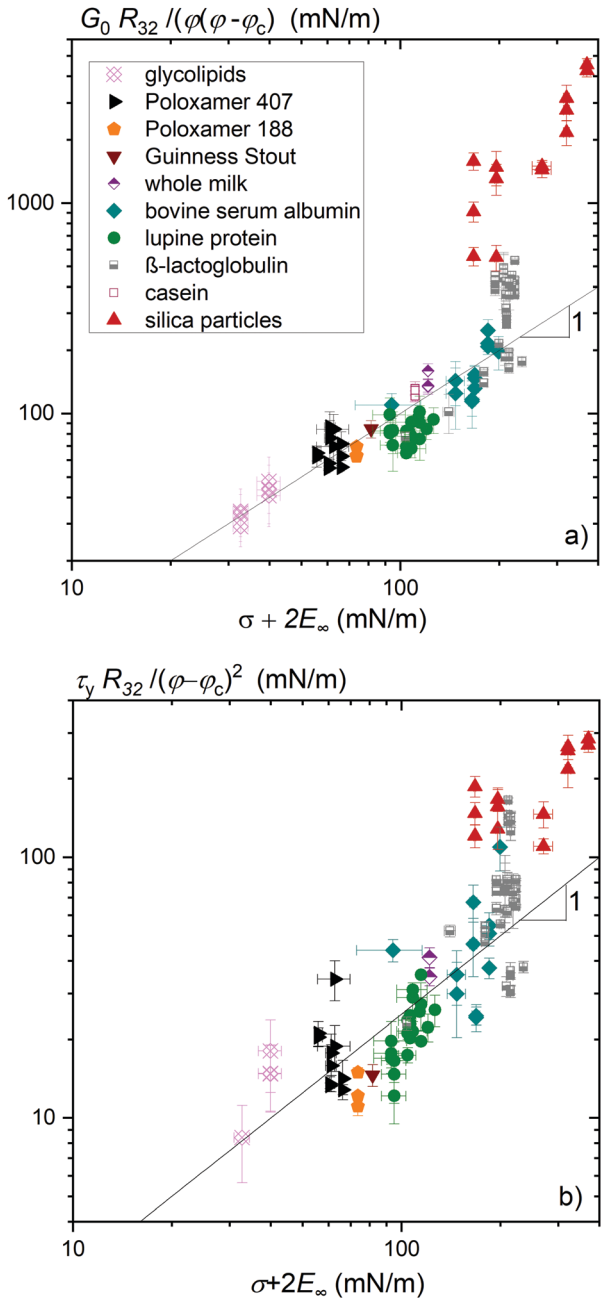

Fig. 3 (a) Foam elastic modulus G_0 normalized by the reciprocal bubble Sauter radius R_{32}^{-1} and $\varphi(\varphi - \varphi_c)$ and (b) foam yield stress normalized by the reciprocal bubble Sauter radius R_{32}^{-1} and $(\varphi - \varphi_c)^2$ *versus* the sum of interfacial tension σ and twice the high frequency elastic modulus E_∞ of the foaming solution in dilation. Solid lines show the linear relationship with the pre-factor $a_d = 1$ in (a) and $k_d = 0.25$ in (b). Data for β-lactoglobulin were reused from ref. 9.

bubble with surface area A

$$\sigma(R) = \sigma_0 + 2E_A \ln\left(\frac{R(t)}{R_0}\right) \quad (7)$$

with the initial interfacial tension σ_0, the initial radius R_0, and the radius $R(t)$ of the dilated bubble.[25] For $\ln(R(t)/R_0) \approx 1$, $\sigma + 2E_\infty$ reflects $\sigma(R)$ in eqn (7). For a sheared foam the

deformation of the gas bubbles is more complex but qualitatively eqn (7) rationalizes why foam modulus and yield stress may scale with $\sigma + 2E_\infty$ and accordingly $(\sigma + 2E_\infty)/R_{32}$ may be termed generalized Laplace pressure.

The correlations shown in Fig. 3(a) and (b) suggest the following model equations:

$$G' = a_d \frac{(\sigma + 2E_\infty)}{R_{32}} \varphi(\varphi - \varphi_c) \quad (8)$$

$$\tau_y = k_d \frac{(\sigma + 2E_\infty)}{R_{32}} (\varphi - \varphi_c)^2 \quad (9)$$

which fit the majority of the data with $a_d = 1$ and $k_d = 0.25$. Note that these pre-factors are slightly smaller than their analogues a in eqn (1) and k in eqn (2) derived for small molecular weight surfactants where E_∞ is neglectable.

However, the extremely high elasticities of foams stabilized by silica particles or aggregated proteins deviate from this scaling. Foam elasticity and yield stress in these cases are obviously not captured by the interfacial tension and its change upon interfacial dilation. They may be dominated by strong attractive forces within the stabilizing surface layers presumably resulting in structures spanning across foam lamellae. This is corroborated by the unusually strong dependence of foam modulus and yield stress on φ observed in these cases, exceeding the well-known scaling $\varphi(\varphi - \varphi_c)$ and $(\varphi - \varphi_c)^2$ observed for many surfactant or protein stabilized foams and emulsions by far. Recently synergetic effects between interfacial elasticity and strong attractive forces among emulsion droplets was reported to lead to high bulk elastic moduli.[26] Such strong attractions among gas bubbles may also contribute to the high elastic modulus and yield stress values as well as their strong dependence on gas volume fraction observed here.

This distinct dependency of the foams' elastic modulus and yield stress on gas volume fraction φ is shown in Fig. 4(a) and (b) for foaming solutions of various ionic strength containing dissolved proteins or particles, respectively. For protein solutions without added salt, the foam elastic modulus increases with $\varphi(\varphi - \varphi_c)$ and yield stress increases with $(\varphi - \varphi_c)^2$ as predicted from model eqn (7) and (8). When the ionic strength of the β-lactoglobulin solution is increased, the foam elastic modulus and yield stress also obey the common φ-scaling but with increased pre-factors a_d and k_d. In case of particle stabilized foams, the elastic modulus and yield stress increase with $\varphi(\varphi - \varphi_c)$ and $(\varphi - \varphi_c)^2$ according to a scaling exponent ≈ 2. Hence our data indicate a stronger increase of foam elastic modulus and yield stress during drainage of foams stabilized by hydrophobized silica nanoparticles and under conditions allowing for a denser packing of the foaming agents at the interface, as it is the case for proteins at high ionic strength of the solution. Such protein aggregates are frequently considered as 'nanoparticles' and form highly stable foams since they are partially hydrophobic and small enough (<70 nm for β-lactoglobulin) to adsorb onto the interface.[27,28] In former studies, high foam elasticity was attributed to interlamellar network formation of aggregated proteins.[9,20]

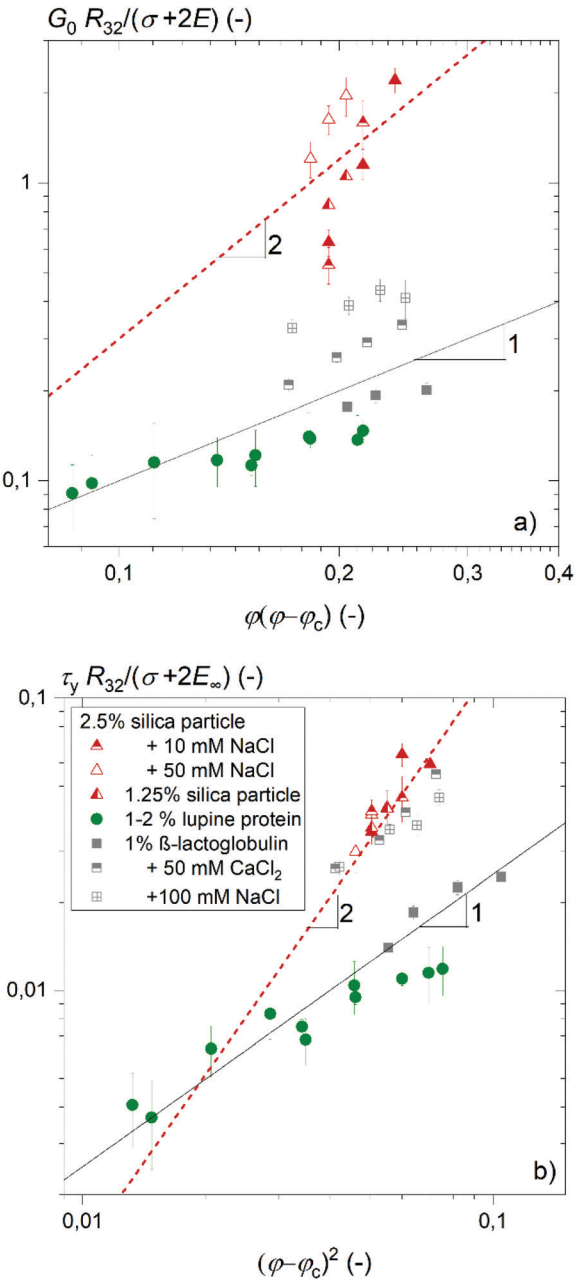

Fig. 4 (a) Foam elastic modulus and (b) foam yield stress normalized by $(\sigma + 2E_\infty)/R_{32}$ *versus* $\varphi(\varphi - \varphi_c)$ and $(\varphi - \varphi_c)^2$, respectively. Solid lines show a linear dependence and dashed lines show a quadratic dependence. Data for β-lactoglobulin were reused from ref. 9.

Accordingly, the stronger increase of the elastic modulus and yield stress with increasing gas volume fraction could be explained by compaction of these networks when the lamellae narrow down.

Conclusions

We investigated close packed aqueous foams stabilized by a broad variety of amphiphiles, including glycolipid surfactants, block copolymers, plant- and animal-based proteins, as well as

nanoparticles, in order to elucidate the coupling between foam flow and the interfacial elasticity of the corresponding amphiphile solution.

We measured the shear modulus G_0 and yield stress τ_y of foams at various gas volume fractions φ and determined the mean Sauter diameter R_{32} simultaneously. Interfacial elasticity was characterized in terms of dilatational as well as shear modulus E_∞ and G_i', respectively.

Our data cover more than two orders of magnitude regarding the absolute values of foam shear modulus, yield stress and interfacial elastic moduli.

In line with previous investigations foam modulus and yield stress strongly vary with interfacial elasticity.

Foams stabilized by nanoparticles and certain protein solutions exhibit a pronounced interfacial shear elasticity, but the range of linear response is narrow, indicating strong attractive interactions or jamming of particles in the surface layer. In these cases the foam modulus scales as $G_0 = a_s[(\sigma + 2G_i)/R_{32}](\varphi(\varphi - \varphi_c))$ with $a_s = 1.6$ and for vanishing elasticity reduces to the well-known model presented in eqn (1) confirmed for numerous foams and emulsions stabilized by low molecular weight surfactants.

Dilatational elasticity of foaming solutions could be determined for all investigated systems also including the glycolipid surfactants and block-copolymers.

For this comprehensive data set scaling laws $G_0 = a_d[(\sigma + 2E_\infty)/R_{32}](\varphi(\varphi - \varphi_c))$ and $\tau_y = k_d[(\sigma + 2E_\infty)/R_{32}](\varphi - \varphi_c)^2$ are confirmed. The numerical pre-factors $a_d = 1$ and $k_d = 0.25$, however, deviate from those reported in the literature for various foam and emulsion systems based on amphiphiles without measurable dilatational elasticity. The term $(\sigma + 2E_\infty)/R_{32}$ represents a generalized Laplace pressure and characterizes the change of surface tension with deformation.

Substantial deviations from this simple scaling were, however, observed for systems either stabilized by hydrophobic silica nanoparticles or by β-lactoglobulin aggregated at high ionic strength or at the isoelectric point. In these cases, strong attractive interactions among particles or particulate protein molecules are present and even structure formation across the foam lamellae may occur which strongly contribute to the foam modulus and yield stress but do not show up in E_∞. This hypothesis is further supported by the previously not reported strong dependence of normalized modulus or yield stress on gas volume fraction found for these systems.

The strong correlation between bulk and interfacial elasticity for close packed foams and the empirical scaling laws found to be valid for a broad range of different foam forming amphiphiles may stimulate further theoretical work providing a deeper understanding of these phenomena which are of significant technical relevance.

Conflicts of interest

There are no conflicts to declare.

Appendix

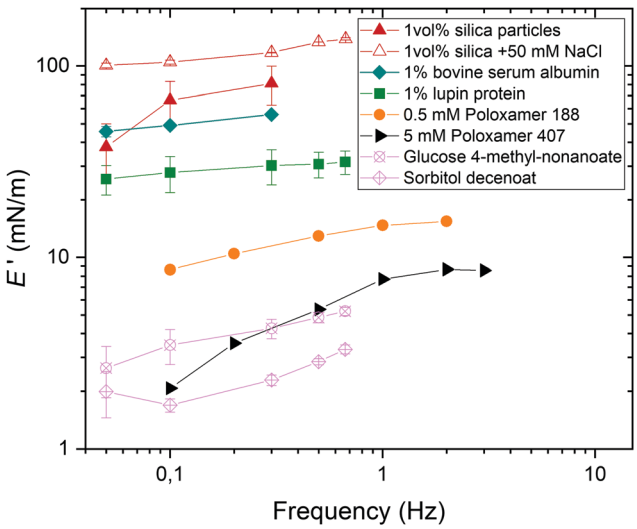

Fig. 5 Frequency dependence of the interfacial elastic modulus measured in oscillatory dilation at deformation amplitudes in the linear viscoelastic regime.

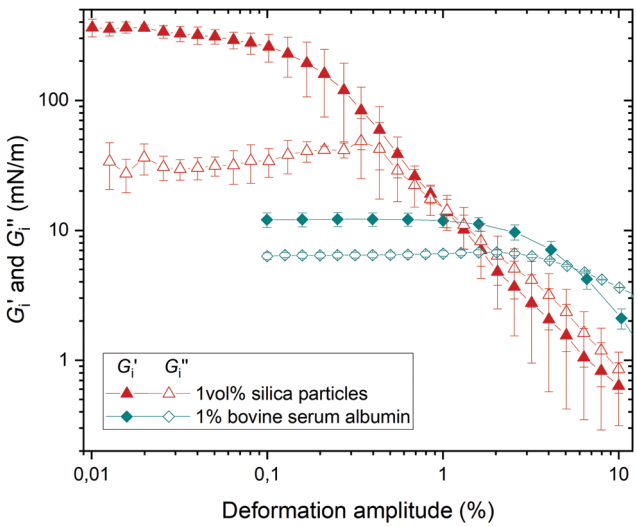

Fig. 6 Strain dependence of interfacial storage modulus G_i' and loss modulus G_i'' measured in oscillatory shear at a frequency of 1 Hz.

Acknowledgements

We thank the groups of W. Drenckhan (Institut de Chimie, Institut Charles Sadron, France) and H. Karbstein (Institute of Process Engineering in Life Sciences I: Food Process Engineering, Karlsruhe Institute of Technology, Germany) for access to their oscillating drop tensiometers and the group of M. Wilhelm (Institute for Chemical Technology and Polymer Chemistry, Karlsruhe Institute of Technology, Germany) for access to their rotational rheometer and the double wall ring geometry. We acknowledge the funding by the DFG project "Rheology and

structural properties of protein and particle-stabilized foams – a multi-scale approach'' WI 3138/29-1.

Notes and references

1 H. M. Princen, *J. Colloid Interface Sci.*, 1982, **91**, 160–175.
2 H. M. Princen, *J. Colloid Interface Sci.*, 1979, **71**, 55–66.
3 H. M. Princen and A. D. Kiss, *J. Colloid Interface Sci.*, 1986, **112**, 427–437.
4 T. G. Mason, J. Bibette and D. A. Weitz, *Phys. Rev. Lett.*, 1995, **75**, 2051–2054.
5 T. G. Mason, J. Bibette and D. A. Weitz, *J. Colloid Interface Sci.*, 1996, **179**, 439–448.
6 S. Marze, R. M. Guillermic and A. Saint-Jalmes, *Soft Matter*, 2009, **5**, 1937–1946.
7 T. D. Dimitrova and F. Leal-Calderon, *Adv. Colloid Interface Sci.*, 2004, **108–109**, 49–61.
8 J. P. Davis, E. A. Foegeding and F. K. Hansen, *Colloids Surf., B*, 2004, **34**, 13–23.
9 M. Lexis and N. Willenbacher, *Soft Matter*, 2014, **10**, 9626–9636.
10 S. Tsibranska, S. Tcholakova, K. Golemanov, N. Denkov, E. Pelan and S. D. Stoyanov, *J. Colloid Interface Sci.*, 2020, **564**, 264–275.
11 S. Costa, R. Höhler and S. Cohen-Addad, *Soft Matter*, 2013, **9**, 1100.
12 S. Vandebril, A. Franck, G. G. Fuller, P. Moldenaers and J. Vermant, *Rheol. Acta*, 2010, **49**, 131–144.
13 G. Lin, J. M. Frostad and G. G. Fuller, *Phys. Rev. Fluids*, 2018, **3**, 114001.
14 S. Cohen-Addad, R. Höhler and O. Pitois, *Annu. Rev. Fluid Mech.*, 2013, **45**, 241–267.
15 N. Pagureva, S. Tcholakova, K. Golemanov, N. Denkov, E. Pelan and S. D. Stoyanov, *Colloids Surf., A*, 2016, **491**, 18–28.
16 R. Hollenbach, A. R. Völp, L. Höfert, J. Rudat, K. Ochsenreither, N. Willenbacher and C. Syldatk, *Molecules*, 2020, **25**, 3797.
17 A. R. Völp, L. Kagerbauer, J. Engmann, D. Z. Gunes, C. Gehin-Delval and N. Willenbacher, *J. Food Eng.*, 2020, **290**, 110150.
18 A. R. Völp, J. Seitz and N. Willenbacher, *Food Hydrocoll.*
19 A. Carl, A. Bannuscher and R. Von Klitzing, *Langmuir*, 2015, **31**, 1615–1622.
20 M. Lexis and N. Willenbacher, *Colloids Surf., A*, 2014, **459**, 177–185.
21 K. Feitosa, S. Marze, A. Saint-Jalmes and D. J. J. Durian, *J. Phys.: Condens. Matter*, 2005, **17**, 6301.
22 A. R. Völp, F. Fessler, J. Reiner and N. Willenbacher, *Chem. Eng. Technol.*, 2020, **43**, 1897–1902.
23 R. H. Ewoldt, M. T. Johnston and L. M. Caretta, *Experimental Challenges of Shear Rheology: How to Avoid Bad Data*, Springer, New York, 2015.
24 N. Willenbacher and M. Lexis, *Foam Films and Foams: Fundamentals and Applications*, CRC Press, Boca Raton, 2018.
25 W. Kloek, T. Van Vliet and M. Meinders, *J. Colloid Interface Sci.*, 2001, **237**, 158–166.
26 S. Tsibranska, S. Tcholakova, K. Golemanov, N. Denkov, L. Arnaudov, E. Pelan and S. D. Stoyanov, *Food Chemistry*, 2020, **316**, 126365.
27 B. S. Murray and R. Ettelaie, *Curr. Opin. Colloid Interface Sci.*, 2004, **9**, 314–320.
28 A. L. Fameau and A. Salonen, *C. R. Phys.*, 2014, **15**, 748–760.